文章编号：1001-9014(2020)04-0422-08

DOI:10.11972/j.issn.1001-9014.2020.04.005

Investigation of low-voltage broadband overmoded folded rectangular coaxial waveguide TWT at W-band

XU Duo[1], WANG Shao-Meng[2], SHAO Wei[1], HE Teng-Long[1], WANG He-Xin[1], TANG Tao[1], GONG Hua-Rong[1], LU Zhi-Gang[1], WANG Zhan-Liang[1], DUAN Zhao-Yun[1], WEI Yan-Yu[1], FENG Jin-Jun[3], GONG Yu-Bin[1*]

(1. School of Electronic Science and Engineering, University of Electronic Science and Technology of China, Chengdu 610054, China;
2. Satellite Research Centre, Nanyang Technological University, Singapore 639798;
3. Beijing Vacuum Electronics Research Institute, Beijing 100015, China)

Abstract: To develop high frequency, broad bandwidth and low voltage traveling wave tube (TWT), the folded rectangular coaxial waveguide slow wave structure (FRCW-SWS) is proposed in this paper. Operating at overmoded condition, the proposed FRCW-SWS has relatively high operating frequency and acceptable transmission characteristics. A double ridge-loaded waveguide-to-coaxial-waveguide converter is designed and applied as the input/output coupler to incorporate the broadband characteristics of the FRCW-SWS. The hot performance of this overmoded FRCW-TWT at W-band is investigated using particle-in-cell (PIC) simulation. The simulation results indicate that the output power can be over 13.7 W in the frequency range of 76 ~ 110 GHz, when the length of the SWS, the beam voltage and beam current are 32 mm, 3230 V and 150mA, respectively. The maximal output power is about 27.4 W at the frequency of 108 GHz, corresponding to the RF efficiency of 5.65%.

Key words: overmoded traveling wave tube, planar slow wave structure, broadband amplifier, folded coaxial waveguide

PACS:84.30.Le, 84.40.Fe

W波段低电压宽带过模矩形同轴曲折波导行波管的研究

许 多[1], 王少萌[2], 邵 伟[1], 何腾龙[1], 王禾欣[1], 唐 涛[1], 巩华荣[1], 路志刚[1], 王战亮[1], 段兆云[1], 魏彦玉[1], 冯进军[3], 宫玉彬[1*]

(1. 电子科技大学 电子科学与工程学院,四川 成都 610054;
2. 南洋理工大学 卫星研究中心,新加坡 639798;
3. 北京真空电子技术研究所,北京 100015)

摘要:提出了一种具有高频率、宽频带和低电压特点的矩形同轴曲折波导慢波结构,所提出的矩形同轴曲折波导工作于过模状态,工作频率较高,同时具有不错的传输特性。设计了一种宽带的双脊加载的波导-同轴转换器,其带宽可以覆盖矩形同轴曲折波导行波管的整个工作频带。所设计的矩形同轴曲折波导行波管工作电压和电流分别为3230 V和150 mA,慢波结构长度为32 mm,PIC仿真结果表明,在76~110 GHz频率范围内,其输出功率超过13.7 W,在108GHz频点,输出功率达到最大值,约为27.4 W,对应的射频效率为5.65%。

关 键 词:过模行波管;平面慢波结构;宽带放大器;同轴曲折波导

中图分类号:TN124 **文献标识码**:A

Received date: 2019-07-11, **revised date**: 2020-01-02 **收稿日期**:2019-07-11,**修回日期**:2020-01-02

Foundation items: Supported by National Natural Science Foundation of China (61531010, 61921002), the International Cooperating Project of Sichuan Province (2018HH0132), and the National Key Lab Foundation of China (9140A23010415DZ02001)

Biography: XU Duo (1995-), male, Anqing, China, doctoral candidate. Research area involves planar miniaturized traveling wave tubes and terahertz traveling wave tubes. E-mail: xuduo1234567@hotmail.com

[*] **Corresponding author**: E-mail: ybgong@uestc.edu.cn

Introduction

Traveling wave tube is one type of high efficiency microwave amplifier with wide applications. Since invented at 1940s, it has been used in many microwave and electronic devices, such as radar and satellite communication systems, due to its characteristics of high power, high gain, broad operating band and so on. However, with the increase of operating frequency, the difficulty of processing of the SWS of traditional helix TWT raises rapidly. Thus, many novel SWSs have been proposed by researchers at millimeter wave and submillimeter wave band.

Folded rectangular waveguide (FRW) is a well-known SWS for millimeter wave and submillimeter wave TWTs. In general, FRW-TWT[1-4] can work at high frequency with a high power capacity, but it is not dominant in the bandwidth and operating voltage. Another famous SWS is the planar miniaturized SWS[5-12]. Some of the planar miniaturized SWSs have the characteristics of low voltage, and others may have the advantages of broad bandwidth. But low operating frequency waveband is a common disadvantage of most current planar miniaturized SWSs.

To develop a TWT with high operating frequency, broad bandwidth, and low operating voltage, a novel SWS named FRCW-SWS is proposed in this paper. The proposed novel SWS is set to work at the second order mode to increase the operating frequency and reduce the operating voltage.

Compared to FRW-SWS, the bandwidth of the proposed FRCW-SWS is much broader. Meanwhile, the proposed FRCW-SWS can work at higher frequency waveband than the conventional planar miniaturized SWSs.

The novel FRCW-SWS is formed by folding the rectangular coaxial waveguide along the axial direction. Waveguide input/output port is selected for the W-band FRCW-SWS TWT as it has a higher power capacity. To match the broad bandwidth of FRCW-SWS, a rectangular coaxial waveguide to standard rectangular waveguide converter is designed for the input/output structure.

This paper is organized as follows. Section II gives a detailed description of the novel SWS, explaining the structure and the main parameter. The operation mode and advantages of the novel FRCW-SWS is analyzed in Section III. In addition, Section III gives the high frequency characteristics of the novel SWS. Section IV presents the double-ridges loaded waveguide to rectangular coaxial waveguide converter for the input/output structure of the novel FRCW-SWS. Finally, Section V shows the setting and results of beam-wave interaction simulation.

1 Description of SWS

Coaxial waveguide is known as a type of transmission line containing an inner conductor and a conducting shield. As the electric field distribution in rectangular coaxial waveguide[13] is more suitable for beam-wave interaction than that of a circular coaxial waveguide, the rectangular coaxial waveguide is adopted to form a SWS by folding it periodically like conventional rectangular folded waveguide SWS.

Figure 1 shows 3-D models of the proposed folded rectangular coaxial waveguide SWS and the conventional rectangular folded waveguide SWS. Figure 1(a) is the conventional rectangular folded waveguide SWS with a rectangular electron beam tunnel, while Fig. 1 (b) is the proposed FRCW-SWS. The main difference between them is the metal strip marked by green inside the nether one. It should be noted that the green color is just for emphasizing the difference, while in practical the inner conductor is with the same material as the conducting shield.

In consideration of the physical truth, two dielectric poles are placed in the conducting shield to hold the inner conductor. The dielectric poles are made of diamond, with a relative permittivity of 5.68. The FRCW-SWS is a periodic structure and a unit cell can nearly express all structure characteristics. Detailed sketches of one FRCW unit and the diagram of the meander route are shown in Fig. 2.

Figures 2 (a-b) are the main and top views of a single period of outer conductor including dielectric poles of the FRCW-SWS, respectively. There are some straight lines on the sides of meander route, marked as w_2, which are prepared for the wielding sections between inner conductor and dielectric poles.

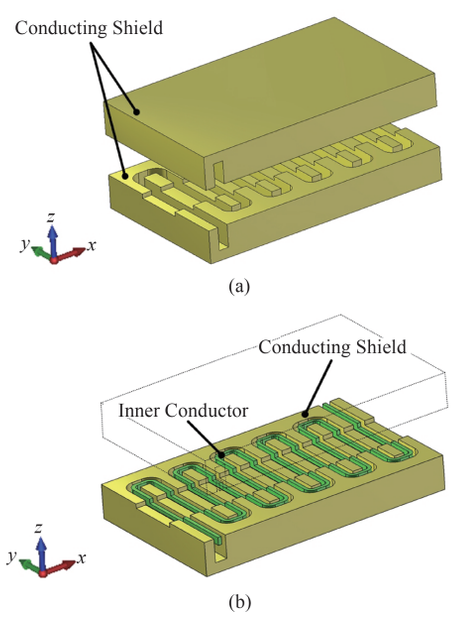

Fig. 1 Sketches of (a) folded rectangular waveguide, and (b) FRCW-SWS
图1 (a)矩形曲折波导和(b)矩形同轴曲折波导的结构示意图

Figures 3 (a-b) are the main and top views of a single period of inner conductor of the FRCW-SWS, respectively. The red dashed area in Fig. 3 (b) is a partial enlarged description. As labeled, *ebtw* and *ebtt* are the width and height of the electron beam tunnel, respectively. l and w_2 are the lengths of transverse straight line and the side straight line of the meander path, respectively. r

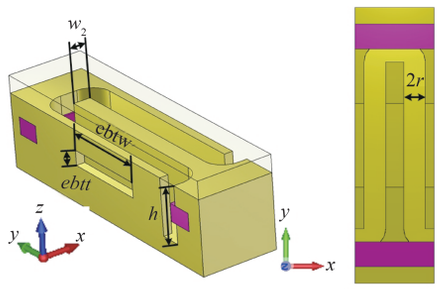

(a) (b)

Fig. 2 (a) The model, and (b) the top view of the conducting shield and the dielectric poles in one period
图2 单周期内金属外壳和介质杆的(a)模型和,(b)俯视图

is the radius of the arc section of the meander path. t and w are the thickness and the width of the inner conductor, respectively. dpt and dpw are the thickness and width of the dielectric pole, respectively.

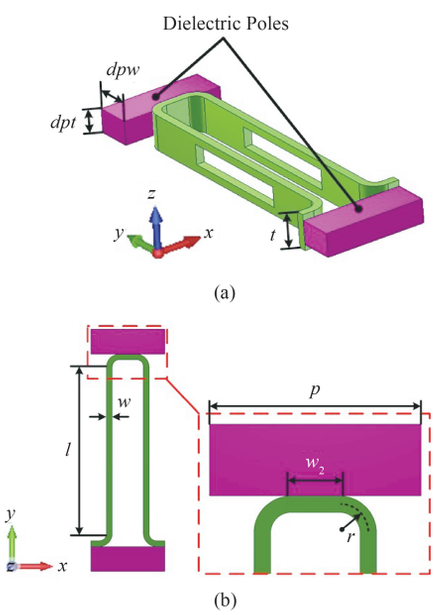

(a)

(b)

Fig. 3 (a) The model and (b) the top view of the inner conductor and the dielectric poles in one period
图3 单周期内金属内导体和介质杆的(a)模型和(b)俯视图

2 High frequency characteristics of FRCW-SWS

2.1 Analyses of operating mode

The FRCW-SWS has many advantages such as broad bandwidth, low operating voltage and high operating frequency. The reasons of these advantages are analyzed as follows.

First, the fundamental mode of the coaxial waveguide is TEM mode while the fundamental mode of the rectangular waveguide is TE_{10} mode. The dispersion characteristics of TEM mode are much weaker than that of TE_{10} mode. As a result, we can predict that the bandwidth of the FRCW-SWS is much broader than that of the FRW-SWS.

In addition, compared to other SWSs working at TEM or Quasi-TEM mode, such as microstrip meander line SWS and strip meander line SWS, the bandwidth of the novel FRCW-SWS is broader. That can be explained by the equivalent circuit[14-18] theory.

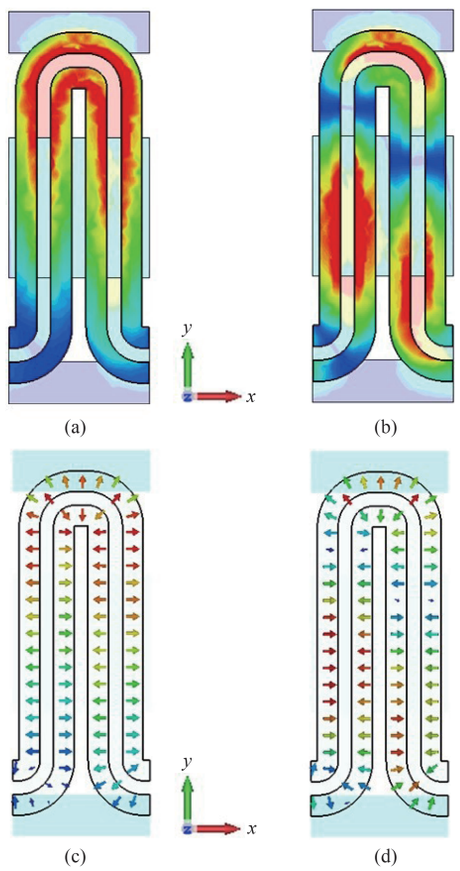

(a) (b)

(c) (d)

Fig. 4 Scalar diagram and vector diagram of electric field intensity distribution of (a,c) the fundamental mode, and (b,d) the second order mode
图4 (a,c)基模和(b,d)二次模的电场强度分布的标量图和矢量图

The addition inductance caused by the coupling among the transverse sections of the inner conductor varies with frequency, which is the main cause of dispersion. The isolation of conducting shield from the transverse sections of the inner conductor reduces the coupling strength of the transverse sections, therefore, the additional inductance of the novel FRCW-SWS is smaller than that of the conventional microstrip meander line SWS or strip meander line. So, the bandwidth of the FRCW-SWS is broader.

The low voltage of the FRCW-SWS can be explained by two aspects. One is that the phase velocity of TEM mode is lower than that of TE_{10} mode.

The other one can be explained as follows. The proposed FRCW-SWS works at overmode state, specifically the second order mode, the corresponding frequency of which is higher. The second order mode is also TEM mode, the same as the fundamental mode, but its frequency is higher, and wavelength is shorter. The wavelength of the fundamental mode is over the length of the

meander path in one period and but the wavelength of the second order mode is shorter than that and over half of that. The electric field distributions of fundamental mode and second order mode are shown in Fig. 4.

According to the relation between the propagation modes and the path length of one single period, in order to make the FRCW-SWS working at the fundamental mode, it requires that the length of meander path in a single period is shorter than the wavelength of the TEM wave propagating along the meander path. It means that when the SWS is working at the fundamental mode, the transverse width is limited to be shorter than a half of the wavelength. But while the SWS works at overmode state, the limit mentioned above could be broken. Thus, the transverse width and aspect ratio are approximately doubled without changing the length of period. These explained the low operating voltage characteristics of the novel FRCW-SWS.

2.2 Dispersion characteristics

The values of the marked parameters in Figs. 2-3 of the designed SWS in this manuscript are optimized and listed in Table 1.

Figure 5(a) shows the dispersion curves of the first two modes on the FRCW-SWS. The simulation results show that the operating voltage of the FRCW-SWS is about 3230 V, for comparison, the operating voltage of the W-band FRW-SWS reported by Ref. 1 is about 16kV. The period length of the FRCW-SWS is about a half of that of the FRW-SWS.

To acquire the dispersion characteristics of the FRCW-SWS with parameters listed in Table 1, a half period model with Master/Slave boundary is built and simulated. The affection of the width w and thickness t of inner conductor on the dispersion curve are studied and shown in Figs. 5 (b-c). The dispersion characteristics have been represented as normalized phase velocity. Figures 5 (b-c) indicate that if we increase w or t and keep the other dimensions stand, it will improve the normalized phase velocity of electromagnetic wave. In addition, the affection of w and t on the coupling impedance are shown in Figs. 5(d-e).

2.3 Interaction impedance

The other significant high frequency characteristic of a SWS is Pierce interaction impedance[19]. It is defined by the relation between the field intensity and power flow in SWS along the longitudinal direction and reflects the interaction strength between charged particles and the longitudinal electric field. To illustrate the Pierce interaction impedance of SWS in the area of cross section of sheet electron beam, 9 points are sampled and interaction impedance on these points are calculated. Figure 6 shows the average value of these 9 sampling points at different frequencies.

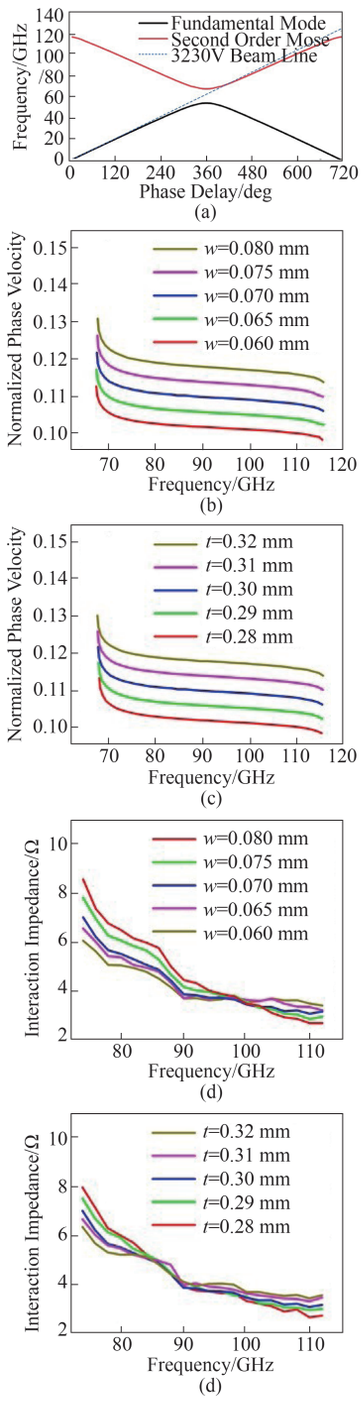

Fig. 5 (a) Dispersion curves of the FRCW-SWS, (b,c) The normalized phase velocities, and (d,e) the interaction impedances of wave in the FRCW-SWS in various w and t of the second order mode

图5 (a)矩形同轴曲折波导慢波结构的色散曲线; 矩形同轴曲折波导慢波结构中二次模的(b,c)归一化相速度和(d,e)耦合阻抗随w和t的变化关系

Table 1 Dimensional parameters of the designed SWS
表1 慢波结构的尺寸参数

Symbol	l	w_2	r	w	t	P	h	$ebtw$	$ebtt$	dpw	dpt
Value/mm	2	0.07	0.1	0.07	0.3	0.54	0.64	1	0.17	0.2	0.2

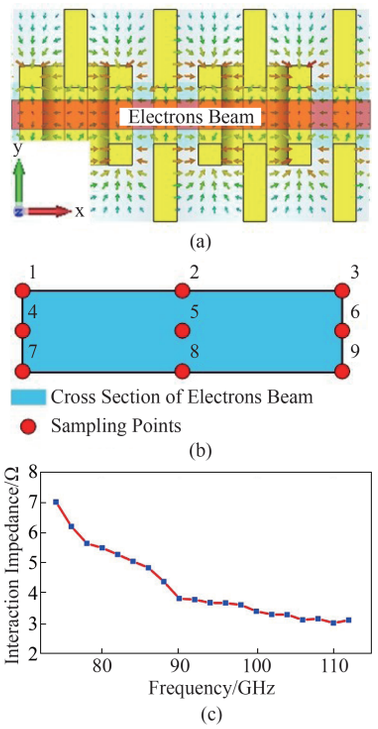

Fig. 6 (a) The position of electron beam in the SWS, (b) the distribution of sampling points in the cross section of the electron beam, and (c) average pierce interaction impedance in the cross section of the electron beam

图6 (a)慢波结构中电子注的位置,(b)电子注横截面上采样点的分布,(c)电子注横截面上的平均耦合阻抗

3 Rectangular waveguides to coaxial waveguide converter

Rectangular waveguide to coaxial waveguide or coaxial waveguide to rectangular waveguide transition is a valuable question of microwave transmission field and has been investigated by many researchers. There are multifarious theories[20-21] and designs[22-23] about the transition.

In order to cooperate the proposed broadband SWS, a broadband double-ridges loaded waveguide to rectangular coaxial waveguide converter is developed.

The converter contains two transitions in fact. One is rectangular coaxial waveguide to double-ridges loaded waveguide and the other one is double-ridges loaded waveguide to W-band standard rectangular waveguide (WR-10). Figure 7 is the diagram of the converter.

The optimized values of structure parameters are listed in Table 2 and the corresponding transmission characteristics are provided by Fig. 8. The rectangular coaxial waveguide port is set as input port (Port 1) and the standard rectangular waveguide port is set as output port (Port 2).

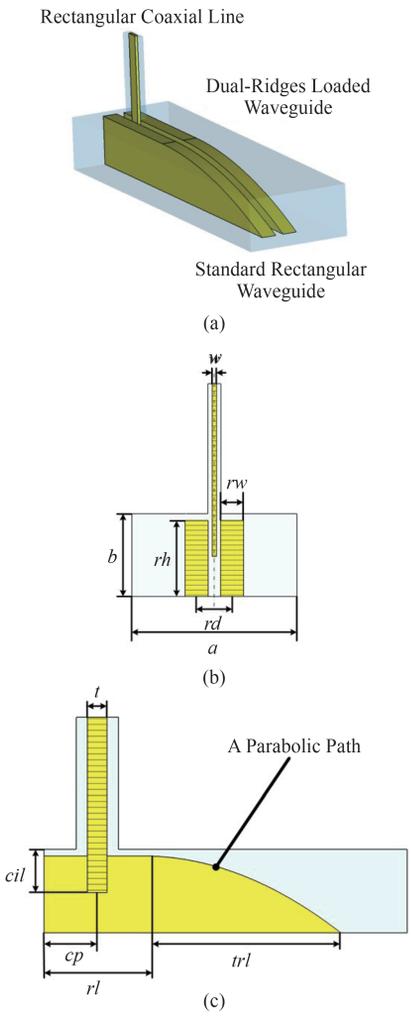

Fig. 7 (a) The model, (b) the front cross section view, and (c) the side cross section view of the rectangular coaxial waveguide to rectangular waveguide converter

图7 矩形同轴波导到矩形波导转换器的(a)模型,(b)正截面图,(c)侧截面图

As can be seen, the designed converter has a prominent performance of broad band. At the frequency range of 74 ~ 113 GHz, the return loss of converter stands below -20dB and the insertion loss is less than -0. 5 dB.

Then, a pair of the proposed converter are assembled with a section of 33-periods FRCW-SWS as the input/output structure, as shown in Fig. 9 (a). The corresponding simulated *S*-parameters are shown in Fig. 9 (b). S_{11} stands below -10 dB and S_{21} stands over -10 dB at the frequency range of 73 ~ 112 GHz.

In the simulation, all the metal parts are set as oxygen free copper. Considering the influence of surface roughness to the conductivity of metal at W-band, the copper conductivity is considered to be $\sigma = 2.2\times10^7$ S/m.

Table 2 Dimensional parameters of the designed converter
表2 转换器的尺寸参数

Symbol	*a*	*b*	*rd*	*rw*	*rl*	*rh*	*trl*	*cp*	*cil*
Value/mm	2. 54	1. 27	0. 545	0. 353	3	1. 168	15	0. 808	0. 610

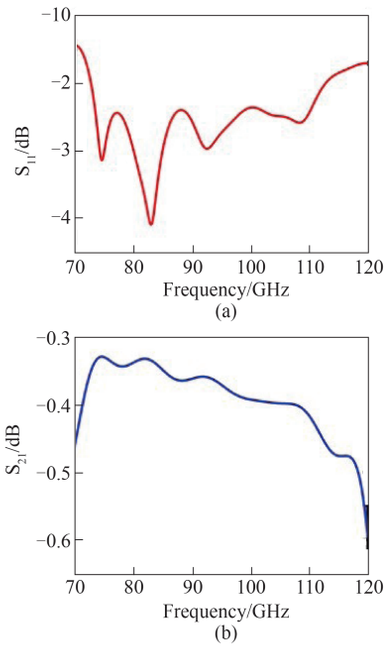

Fig. 8 (a) Return loss, and (b) insertion loss of the converter
图 8 转换器的(a)回波损耗，(b)插入损耗

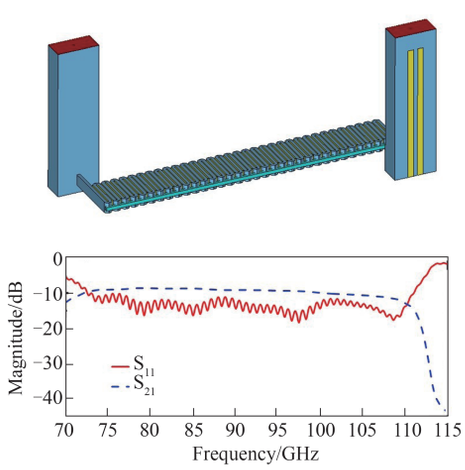

Fig. 9 The transmission characteristics of the FRCW slow wave system with the converters
图 9 带有转换器的矩形同轴曲折波导慢波系统的传输特性

4 Beam-wave interaction simulation

To verify the hot performance of the designed SWS, the beam-wave interaction has been investigated using CST-Particle Studio. To reduce the simulation time and promote the accuracy of calculation, the converters were not included in the PIC simulation.

In the interest of avoiding band edge oscillation, the TWT is truncated into two segments. The numbers of periods are 24 and 33 in in part 1 and part 2, respectively. The overall length of this TWT in 32 mm. The PIC simulation model and its transmission characteristics are shown in Fig. 10.

It is worth noting that the Port 3 and Port 4 are reserved for connecting to coaxial attenuator to depress band edge oscillation. In the simulation, they are set as waveguide ports to extract redundant electromagnetic energy.

In order to explore the capability of the proposed SWS, an ideal sheet electron beam generated by a rectangular electron emitter and a presupposed longitudinal uniform focusing magnetic field are used instead of real electron beam and magnetic field in the simulation. Figure. 11 presents the diagram of the electron emitter and magnetic field distribution.

The emission area is set to 0.9 mm × 0.07 mm and the intensity of the required presupposed longitudinal uniform magnetic field is about 1T. In this case, the presupposed magnetic field can restrict the electrons in electron beam tunnel effectively and no electron is observed hitting at the end side of the SWS.

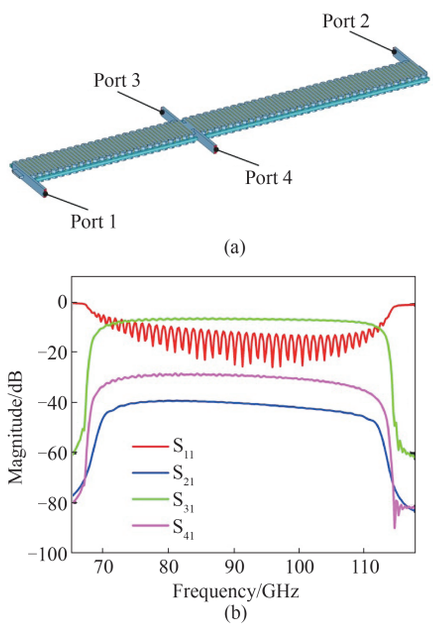

Fig. 10 (a) The sketch and (b) the transmission characteristics of the truncated FRCW-SWS without the converters
图 10 无转换器且已截断的矩形同轴曲折波导慢波结构的(a)结构示意图，(b)传输特性

The operating condition of the simulated TWT is enumerated in Table 3.

Table 3 Operating condition of the designed TWT
表 3 行波管的工作条件

Parameter	Value
Beam Voltage	3230 V
Beam Current	0.15 A
Beam Cross Section	0.9 mm × 0.07 mm
Longitudinal Magnetic Field	1T
Input Power	45 mW

For acquiring the ability of TWT to amplify the power of electromagnetic wave, sinusoidal signal was used as input signal of TWT to drive it. Figure 12 (a) shows input and output signals at 108 GHz. No oscillation was ob-

served in the simulation duration of 30ns. Fig. 12(b) indicates that the frequency spectrum of output signal is quite pure, and no obvious high-order harmonics were noticed. Figure 12 (c) shows the kinetic energy distribution, showing clear beam bunching in the beam-wave interaction.

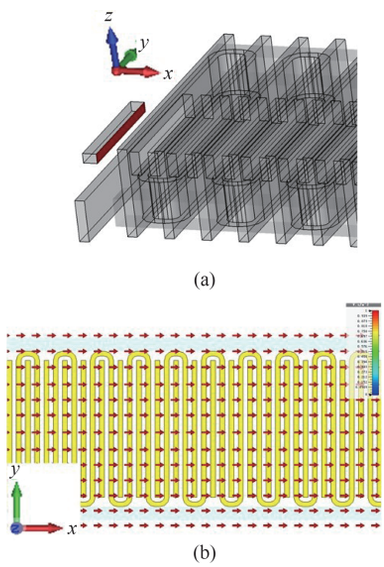

Fig. 11 The diagram of (a) ideal rectangular source face of electrons, (b) presupposed longitudinal uniform magnetic field
图11 (b)理想矩形电子发射面和(b)预设的纵向均匀磁场的示意图

Figure 13 shows the output power and gain vary with input frequency. The maximal output power is 27.4 W at the frequency point of 108 GHz, and the corresponding gain and RF efficiency are 27.8dB and 5.65% respectively. Furthermore, in the frequency range between 76 GHz to 110 GHz, the output power exceeds 13.7 W, and the consequence demonstrated that the 3-dB bandwidth of the TWT is 36.56% centered at 93GHz.

5 Conclusion

A novel SWS named FRCW-SWS was proposed in this paper. The high frequency characteristics were calculated by using HFSS. The simulation results showed that it has a much broader operating bandwidth than conventional FRW-SWSs and miniaturized planar SWSs.

In addition, a double-ridges loaded rectangular coaxial line to standard rectangular waveguide of W-band (WR-10) converter is presented and designed in this paper. The simulation results show that the designed converter can transform the mode of electromagnetic wave effectively.

In general, the operating bandwidths of the reported W-band FRW-TWTs are less than 15% and their operating voltage is about 20 kV. The PIC simulation results in CST indicate that the bandwidth of the novel TWT is 36.56% centered at 93GHz and the operating voltage is 3230 V. That illuminates that the novel overmode FRCW-TWT has clear advantages in the aspects of bandwidth and operating voltage than FRW-TWT. In addition, the maximal output power, gain and RF efficiency of the novel TWT are 27.4 W, 27.8 dB and 5.65% respectively.

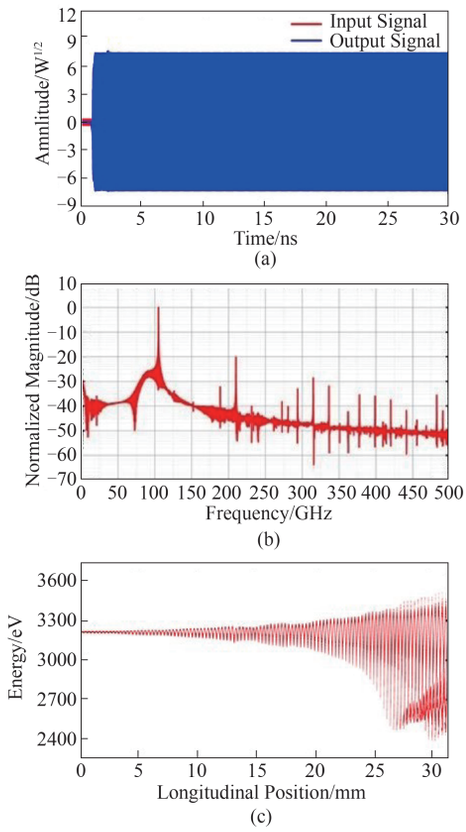

Fig.12 (a) The amplitudes of input and output, (b) the frequency spectrum of output signal, (c) the distribution of the kinetic energy of electrons along with different longitudinal position
图12 (a)输入输出信号的幅值,(b)输出信号的频谱,(c)电子动能随纵向位置的分布

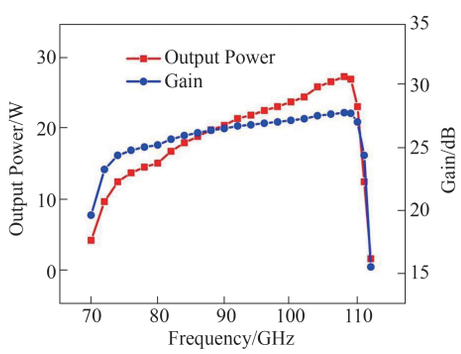

Fig. 13 Output power and gain of the FRCW-TWT with 45 mW sinusoidal signal as input signal
图13 输入45 mW正弦信号时矩形同轴曲折波导行波管的输出功率和增益

References

[1] Sharma R K, Grede A, Chaudhary S, *et al*. Design of folded waveguide slow-wave structure for W-Band TWT [J]. *IEEE Transactions on Plasma Science*, 2014, **42**(10): 3430-3436.
[2] Feng J J, Cai J, Hu Y F, *et al*. Development of W-band folded wave-

guide pulse TWTs [J]. *IEEE Transactions on Electron Devices*, 2014, **60**(6): 1721-1725.
[3] Wei Y Y, Guo G, Gong Y B, *et al*. Novel W-band ridge-loaded folded waveguide traveling wave tube [J]. *IEEE Electron Device Letters*, 2014, **35**(10): 1058-1060.
[4] Cai J, Feng J J, Hu Y F, *et al*. 10 GHz Bandwidth 100 Watt W-band folded waveguide pulsed TWTs [J]. *IEEE Microwave and Wireless Components Letters*, 2014, **24**(9): 620-621.
[5] Liu L W, Wei Y Y, Shen F, *et al*. A Novel Winding Microstrip meander-line slow wave structure for V-band TWT [J]. *IEEE Electron Device Letters*, 2013, **34**(10): 1325-1327.
[6] Chua C, Aditya S. A 3-D U-shaped meander-line slow-wave structure for traveling-wave-tube applications [J]. *IEEE Transactions on Electron Devices*, 2013, **60**(3): 1251-1256.
[7] Chua C, Aditya S, Shen Z X, *et al*. Design of a planar helix with straight-edge connections for traveling-wave tube applications [C]. 2011 IEEE International Vacuum Electronics Conference (IVEC), Bangalore, India, 2011: 207-208.
[8] Bai N F, Gu L L, Shen C S, *et al*. S-shaped microstrip meander-line slow-wave structure for W-band traveling-wave tube [C]. 2013 IEEE 14th International Vacuum Electronics Conference (IVEC), Paris, France, 2013: 1-2.
[9] Ulisse G, Krozer V. Investigation of a planar metamaterial slow wave structure for traveling wave tube applications [C]. 2017 Eighteenth International Vacuum Electronics Conference (IVEC), London, UK, 2017: 1-2.
[10] Benedik A I, Rozhnev, Ryskin N M, *et al*. Planar V-Band Slow-Wave Structures for Low-Voltage Tubes with Sheet Electron Beam [C]. 2017 Eighteenth International Vacuum Electronics Conference (IVEC), London, UK, 2017: 1-2.
[11] Wang S M, Gong Y B, Hou Y, *et al*. Study of a log-periodic slow wave structure for Ka-band radial sheet beam traveling wave tube [J]. *IEEE Transactions on Plasma Science*, 2013, **41**(8): 2277-2282.
[12] Wang H X, Wang Z L, Li X Y, *et al*. Study of a miniaturized dual-beam TWT with planar dielectric-rods-support uniform metallic meander line [J]. *physics of plasmas*, 2018, **25**(6).
[13] Cho Y H, Eom H J. Fourier transform analysis of a ridge-waveguide and a rectangular coaxial line [J]. *Radio Science*, 2001, **36**(4): 533-538.
[14] Booske J H, Converse M C, Kory C L, *et al*. Accurate parametric modeling of folded waveguide circuits for millimeter-wave traveling wave tubes [J]. *IEEE Transactions on Electron Devices*, 2005, **52**(5): 685-694.
[15] Sumathy M, Vinoy K J, Datta S K. Analysis of ridge-loaded folded-waveguide slow-wave structures for broadband traveling-wave tubes [J]. *IEEE Transactions on Electron Devices*, 2010, **57**(6): 1440-1446.
[16] Hou Y, Gong Y B, Xu J, *et al*. A novel ridge-vane-loaded folded-waveguide slow-wave structure for 0.22 THz traveling-wave tube [J]. *IEEE Transactions on Electron Devices*, 2013, **60**(3): 1228-1235.
[17] Pyle J R. The cutoff wavelength of the TE_{10} mode in ridged rectangular waveguide of any aspect ratio [J]. *IEEE Transactions on Microwave Theory and Techniques*, 1966, **14**(4): 175-183.
[18] Pozar D M. *Microwave engineering* [M]. 3rd edition. New York, NY, USA: John Wiley & Sons, 2004.
[19] WANG Wen-Xiang. Microwave Engineering Technology (in Chinese) [M]. 2nd edition. Beijing, China: National Defense Industry Press(王文祥. **微波工程技术**. 国防工业出版社(第二版)), 2009.
[20] Williamson A G. Analysis and modeling of a coaxial-line/rectangular-waveguide junction [J]. *IEE Proceedings H-Microwaves, Optics and Antennas*, 1982, **129**(5): 271-277.
[21] Saad S M. A more accurate analysis and design of coaxial-to-rectangular waveguide and launcher [J]. *IEEE Transactions on Microwave Theory and Techniques*, 1990, **38**(2): 129-134.
[22] Keam R B, Williamson. Broadband design of coaxial line/rectangular waveguide probe transition [J]. *IEE Proceedings - Microwaves, Antennas and Propagation*, 1994, **141**(1): 53-58.
[23] Rudakov V A, Sledkov V A, Mayorov A P, *et al*. Compact wide-band coaxial-to waveguide microwave transactions for X and Ku bands [C]. 2013 IX Internatioal Conference on Antenna Theory and Techniques, Odessa, Ukraine, 2013: 522-523.